Nuclear Technology

ISSN: 0029-5450 (Print) 1943-7471 (Online) Journal homepage: https://www.tandfonline.com/loi/unct20

Surface Characterization of Depleted Uranium–Molybdenum to Determine Surface Coating Compatibility

Terry A. Ring, Byung Sang Choi, J. Paulo Perez, Brian Van Devener, Randy C. Polson, Douglas Crawford, Dennis Keiser & Daniel Wachs

To cite this article: Terry A. Ring, Byung Sang Choi, J. Paulo Perez, Brian Van Devener, Randy C. Polson, Douglas Crawford, Dennis Keiser & Daniel Wachs (2019) Surface Characterization of Depleted Uranium–Molybdenum to Determine Surface Coating Compatibility, Nuclear Technology, 205:6, 801-818, DOI: 10.1080/00295450.2018.1542252

To link to this article: https://doi.org/10.1080/00295450.2018.1542252

Published online: 27 Dec 2018.

NUCLEAR TECHNOLOGY · VOLUME 205 · 801–818 · JUNE 2019

DOI: https://doi.org/10.1080/00295450.2018.1542252

Surface Characterization of Depleted Uranium–Molybdenum to Determine Surface Coating Compatibility

Terry A. Ring,[a]* Byung Sang Choi,[b] J. Paulo Perez,[c] Brian Van Devener,[c] Randy C. Polson,[c] Douglas Crawford,[d] Dennis Keiser,[d] and Daniel Wachs[d]

[a]*University of Utah, Chemical Engineering Department, Salt Lake City, Utah 84112*
[b]*Chosun University, Materials Science and Engineering Department, Gwangju 61452, Korea*
[c]*University of Utah, Surface Analysis Laboratory, Salt Lake City, Utah 84112*
[d]*Idaho National Laboratory, 2525 Fremont Avenue, P.O. Box 1625, Idaho Falls, Idaho 83415*

Received June 12, 2018
Accepted for Publication October 26, 2018

Abstract — *Scanning electron microscopy, transmission electron microscopy, and X-ray photoelectron spectroscopy have been used to characterize the surface of depleted uranium molybdenum (DU-Mo) alloys as a chemical surrogate to determine potential challenges with the surfaces of manufactured and stored U-Mo foils and powders. Even when stored and shipped in an inert atmosphere, U-Mo has a tenacious surface contamination of oxygen and carbon. The 8 at. % molybdenum (DU-8Mo) powder and 10 at. % molybdenum (DU-10Mo) foil samples have surface contamination of oxygen and carbon in different ratios that is hundreds to thousands of nanometers thick. The DU-8Mo powder sample has been stored in an inert atmosphere and as a result has a lower carbon-to-oxygen ratio at the surface than the DU-10Mo foil sample that was stored in air. This surface contamination has not been removed by up to 20 min of argon ion sputtering nor with 5% hydrogen in argon heat treatment for up to 96 h at 950°C.*

Keywords — *Depleted uranium–molybdenum alloy, surface analysis.*

Note — *Some figures may be in color only in the electronic version.*

I. INTRODUCTION

Low-enriched uranium (LEU) molybdenum alloys with various atomic percent amounts of molybdenum are being considered as the new fuel for research reactors across Europe and the United States as part of the implementation of a reduced enrichment nuclear safeguard. The LEU for this purpose consists of an 8 to 10 at. % mixture of molybdenum with uranium containing 19.75% ^{235}U and 80.25% ^{238}U. Two U-Mo fuel concepts are being developed: One is a monolithic foil of U-Mo with Al cladding, and the other is a dispersion fuel where U-Mo particles are dispersed into Al powder that is then pressed into a compact foil. This alloy has a unique high-temperature crystal structure that accommodates fission products allowing up to 80% burnup.[1] This fuel, in the form of either a powder or a foil, is to be sandwiched between two aluminum plates to form a composite fuel plate that will become part of the reactor core. It is desirable to put a coating on the U-Mo surface to hermetically seal the U-Mo to theoretically deter interdiffusion and still allow for strong attachment to the aluminum matrix and cladding. A good bond between U-Mo and the Al matrix/cladding prevents surface voids where fission gas can concentrate forming blisters at these points at this interface. Blisters will lead to poor heat transfer and undesirable hot spots in the fuel element. Interdiffusion leads to the development of a poor

*E-mail: ring@chemeng.utah.edu

thermal conducting interaction layer of uranium and aluminum. A coating of ZrN is being contemplated for the hermetic seal material for the U-Mo and a good bond between U-Mo and Al matrix/cladding.

A coating that bonds well with the U-Mo surface is one where the lattice mismatch is less than 10%. LEU-Mo in its high-temperature crystal structure can accommodate fission gases in a *Im-3m* cubic crystal structure with a lattice spacing of 0.3848 nm that expands to 12 nm after swelling with a super lattice of 3-nm fission gas bubbles arrayed on the uniform face-centered-cubic (fcc) lattice of LEU-Mo crystal structure.[1–3] It will be very difficult for a tenaciously attached coating to accommodate such a large amount of swelling during the accumulation of fission gases although thin, submicron coatings have been shown to be the more resilient to shear stresses. ZrN is a cubic crystal structure with a unit cell of 0.4575 nm. Thus, in principle, it is feasible to have a thin, strongly bound, hermetic coating of ZrN on the initial LEU surface if and only if the LEU surface has been nitrided before coating with ZrN since UN has a fcc lattice with a lattice spacing of 0.438887 nm and Mo_2N has a cubic lattice with a lattice spacing of 0.4220 nm.

X-ray photoelectron spectroscopy (XPS), scanning electron microscopy (SEM), and transmission electron microscopy (TEM) are used to investigate the "as-received" surfaces of 10 at. % molybdenum [depleted uranium (DU)-10Mo] foil and 8 at. % molybdenum (DU-8Mo) powder materials that are surrogates for LEU-Mo nuclear fuel. XPS, SEM, and TEM are also used to investigate various effects from argon ion sputtering and hydrogen heat treatments to remove surface contamination before coating work begins.

II. MATERIALS AND METHODS

Depleted uranium with DU-10Mo foil was obtained from Idaho National Laboratory's (INL's) Y-12 facility. The sample arrived in a plastic bag without additional packaging. The foil had an appearance of dark gray, bordering on black. DU-8Mo powder with a reported size range from 58 to 98 μm was also obtained from INL's Y-12 facility. The DU powder sample arrived in a doubly sealed glass container with instructions to open in an inert atmosphere to prevent pyrophoric reaction. The DU-8Mo powder had a shiny metallic appearance with some particles being much larger than 100 μm in size. It is unknown under what atmospheric conditions these materials were stored or how long they were stored.

The DU-10Mo foil sample was cut in the laboratory atmosphere into a small sample for XPS. In addition, a 40 × 0.5-cm strip was cut from the foil sample for surface treatment in a quartz tube furnace. The DU-10Mo sample was treated at 950°C (centerline temperature) for various durations up to 96 h in 4.901%H_2/Ar mixture flowing at 0.1 standard liter per minute (SLPM) and 3 bar(a). Several small 2-mm^2 cutout samples located at various reactor axial locations and therefore different furnace temperatures were removed from the large sample for treatment and surface analysis.

The DU-8Mo powder sample consists of a composite sample created at INL from an electroatomization process. The DU-8Mo powder sample upon receipt was stored in a glove box fed with ultra high purity (UHP) compressed nitrogen from Airgas. Samples of the powder were transferred to and from the quartz tube furnace under UHP N_2 gas atmosphere. The DU-8Mo powder samples placed at various axial locations in a quartz-lined tube furnace were treated at 950°C (centerline temperature) for various durations in 4.901%H_2/Ar mixture flowing at 0.1 SLPM and 3 bar(a). Samples located at various axial locations and therefore different furnace temperatures were removed from the furnace and mounted for XPS surface analysis. Removal, storage, and transport of these samples were all done under a UHP-N_2 atmosphere.

Scanning electron microscopy analysis of the as-received samples was performed using a FEI Helios Nanolab 650. The focused ion beam (FIB) aspect of the FEI Helios Nanolab 650 instrument was used to prepare TEM liftout samples after a cap of platinum was deposited.

The liftout samples were taken perpendicular to the surfaces of the powder and foil samples. These TEM samples were analyzed using a JEOL JEM-2800 scanning transmission electron microscope with dual energy-dispersive X-ray spectroscopy (EDS) detectors.

The XPS instrument used for these analyses was a Kratos Axis Ultra XPS, made by Kratos Analytical from Manchester, United Kingdom, using a monochromatic Al source (1486 eV). Low-resolution survey scans are collected with 160-eV pass energy at 200-ms dwell time. High-resolution region scans were performed at 40-eV pass energy, 400-ms dwell time. XPS is a surface-sensitive technique that analyzes the surface of the sample up to an ~10-nm depth. The analysis area studied under the X-ray probe is about 300 × 700 μm. Table I provides a list of material structures,[4] lattice spacings,[4–7] and XPS binding energies[8] for materials of interest to this work. Argon ion sputtering is sometimes performed for various times to further clean the samples' surfaces. In all cases argon ion sputtering was performed at 20 mA at an acceleration

TABLE I

Structural and XPS Binding Energies of Various Materials

Material	Structure	Lattice Spacing (nm)	Binding Energy (eV)[a]
U-Mo	Body-centered-cubic	a = 0.34808 to 0.000324 (at. % Mo)[b]	—
U-10Mo	Body-centered-cubic	a = 0.3848	—
α-U	Orthorhombic	a = 0.2854, b = 0.5587, c = 0.4955	377.3(U-4f 7/2) 388.0(U-4f 5/2)
γ-U	Body-centered-cubic	a = 0.3524	377.2(U-4f 7/2) 388.0(U-4f 5/2)
UO_2	Cubic	a = 0.5740	380.1(U-4f 7/2) 391(U-4f 5/2)
UO_3	Cubic	a = 0.4138	381.6(U-4f 7/2) 387.5(U-4f 5/2)
UN_2	Face-centered-cubic	a = 0.438887	377.4(U-4f 7/2)
α-U_2N_3	Body-centered-cubic	a = 1.0678 to 1.0580	378.5(U-4f 7/2)
UN	Face-centered-cubic	a = 0.4880	378.5(U-4f 7/2)
UC	Cubic	a = 0.526	378 (U-4f 7/2) 282 (C-1s 1/2)[b]
Mo	Body-centered-cubic	a = 0.31466	228.4 (Mo-3d 5/2)
MoN	Hexagonal Cubic	a = 0.572, c = 0.5608 a = 0.4212	228.40(Mo-3d 5/2)
Mo_2N	Cubic	a = 0.4163	228.40(Mo-3d 5/2)
MoO_2	Tetragonal	a = 0.4750, b = 0.5748, c = 0.6485	229.3 (Mo-3d 5/2)
MoO_3	Orthorhombic	a = 0.3963, b = 1.3855, c = 0.369	233.1(Mo-3d 5/2)
Mo_2O_3	Hexagonal-close-packed	a = 0.283, c = 0.4901	229.4(Mo-3d 5/2)
Mo_2C	Orthorhombic	a = 0.4729, b = 0.5197, c = 0.6028	228.1(Mo-3d 5/2)
Zr	Hexagonal-close-packed	a = 0.2331, c = 5.1491	178.7(Zr-3d 5/2)
ZrN	Cubic	a = 0.4575	180(Zr-3d 5/2)
ZrO_2	Monoclinic	a = 0.51597, b = 0.52028, c = 0.53156	184.2(Zr-3d 3/2) 181.9 (Zr-3d 5/2) 530.6 (O 1s 1/2)
ZrC	Cubic	a = 0.4697	178.6(Zr-3d 5/2) 180.6(Zr-3d 3/2) 282.3(C-1s 1/2)
Si	Face-centered-cubic	a = 0.5430710	100.4(Si-2p 1/2) 99.8(Si-2p 3/2)
Si_3N_4	Cubic	a = 0.45675	102(Si-2p 1/2)
SiO_2	Quartz-trigonal	a = 0.49133	103–104(Si-2p 1/2)
Al	Face-centered-cubic	a = 0.40495	73.2(Al-2p 1/2) 72.7(Al-2p 3/2)

[a]XPS line of interest.
[b]This work.

voltage of 4 kV. These sputtering conditions remove from 20 to 40 nm of the surface per minute. Gaussian peak decomposition is used to more clearly identify the components of composite peaks.

III. RESULTS

III.A. SEM Results

The SEM results of the as-received samples are shown in Fig. 1. The DU-8Mo powder sample in Fig. 1a shows a smooth surface. The DU-8Mo powder sample was described as one that was made by metal atomization. Several spherical entities can be observed in Fig. 1b, but these seem to have been amalgamated into larger solid pieces that are major constituents of the as-received sample. This amalgamation leads to internal voids in poorly consolidated areas. The DU-10Mo foil sample, Fig. 1c, shows a rough surface with a small amount of flakes and some obvious cracking. This sample also showed some regions where flakes and smaller cracks were observed as shown in Fig. 1d. The surface cracking suggests that the foil sample

is heavily oxidized with UO_2 (and not UO_3) on the surface as the lattice spacing for UO_2 is more than 10% larger than that of the U-Mo base material, which would cause it to crack during oxidation. The lattice spacing of UO_3 is larger than that of the base U-Mo by less than 10%.

III.B. TEM Analysis

Focused ion beam cutout samples, ~10 μm deep and ~5 μm wide, perpendicular to the surfaces shown in Figs. 1a and 1c, were prepared for the TEM analysis. After thinning to several nanometers thick, these samples were examined by scanning transmission electron microscopy
(S/TEM) using various imaging modes including bright field TEM imaging, dark field S/TEM imaging (S/TEM DF), bright field S/TEM imaging, and secondary electron S/TEM imaging.

III.B.1. S/TEM Analysis of DU-8Mo Powder Sample

Figure 2 shows the TEM images of the thinned DU-8Mo powder samples. Here, we see the platinum layer added to the powder surface to protect the surface during cutout and the tip of the pin that was attached to the platinum layer to facilitate liftout. Below the platinum layer is the depleted uranium–molybdenum (DU-Mo) sample surface.

High-resolution analysis of region 1 (see Fig. 2a) shows a clear interface between the sample and the platinum deposit, Fig. 2b. The high-resolution TEM image of the sample, Fig. 2c, shows the phase contrast image of the lattice resolution of the DU-8Mo powder sample. There is some long-range order, but there is also some long-range disorder in the sample. Figures 2d, 2e, and 2f show the EDS maps of U, Mo, and O, respectively. Uranium and molybdenum are colocated in the same region associated with the bulk sample. The oxygen is shown to be in both the U-Mo sample and the platinum layer. These low-magnification images do not present a very precise spatial distribution of the elements. For this reason, higher-magnification EDS maps of the powder surface were also collected and are shown in Fig. 3.

Figure 3a shows a higher-magnification S/TEM-DF image of the surface of the powder showing a nonuniform cloudy surface. With the EDS maps of the interface, we see that the platinum has diffused into the broken, oxygen-

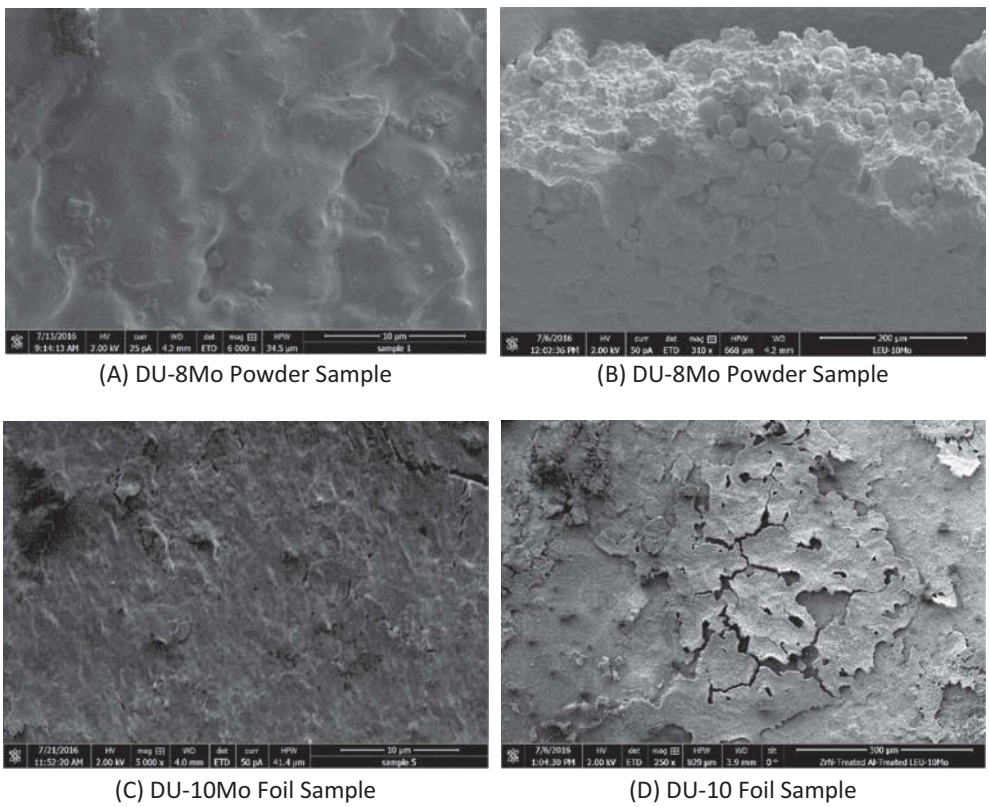

Fig. 1. (a) and (b) SEM of DU-8Mo powder sample surface; (c) and (d) DU-10Mo foil sample surface.

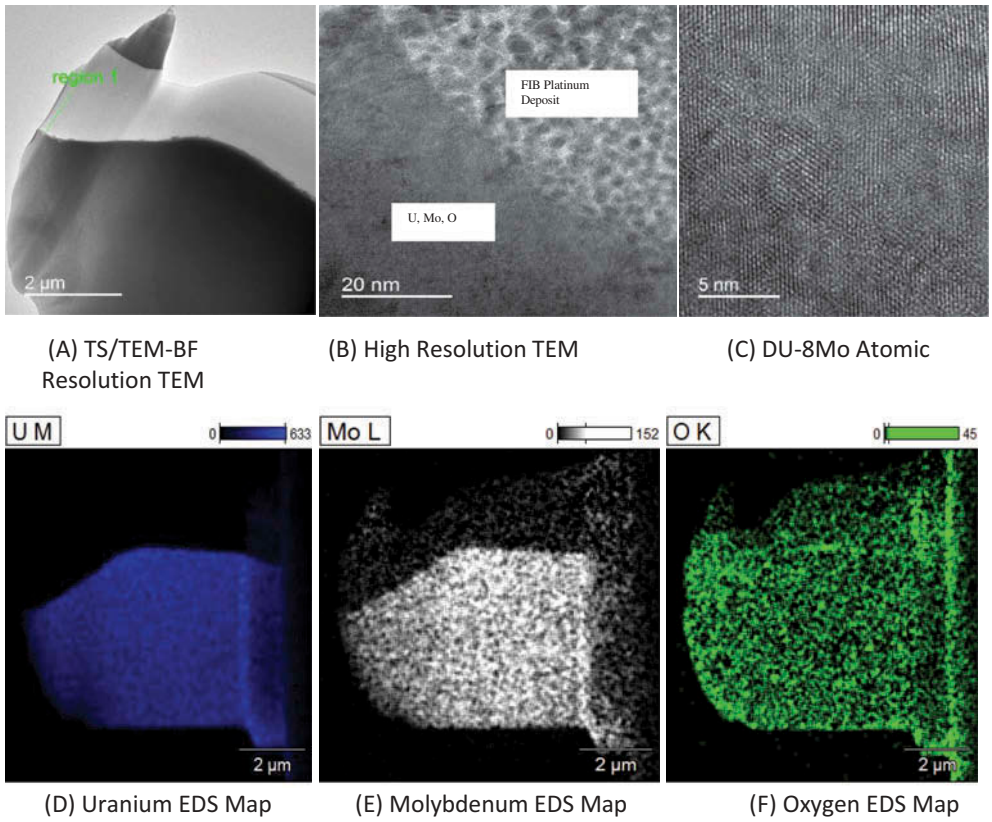

Fig. 2. TEM analysis and EDS maps of as-received DU-8Mo powder sample.

enriched layer. Comparing Fig. 3d with Fig. 3e, molybenum has a presence in the oxygen-enriched layer, more so than the uranium of the bulk sample. An element trace across the interface (Fig. 3f) gives a graded concentration of molybdenum and an oxygen-containing thickness of 130 nm that are similar to those determined from examination of Fig. 3a.

III.B.2. TEM Analysis of DU-10Mo Foil Sample

For the DU-10Mo foil sample, the cutout after thinning is shown in Fig. 4. Here, we see the platinum layer added to the powder surface to protect the surface during cutout, i.e., the black region above the cracked white region in Fig. 4a. Below the platinum layer is the DU-Mo sample surface. The surface is a brighter surface in Fig. 4a indicating a lower-*Z* material, i.e., an oxide layer. This oxide layer is as thick as 2 µm with large cracks protruding up to the sample surface. Below the oxide layer is the U-Mo material. There is a hint of three large (~2 µm) grains of U-Mo metal below the polycrystalline oxide surface in Fig. 4a. High-resolution TEM images of the material shown in the red circle in Fig. 4a are shown in Fig. 4b, and atomic resolution of the material in the red circle in Fig. 4b is shown in Fig. 4c. Multiple crystallites with different crystallographic orientations are shown in Fig. 4c.

Higher-resolution EDS maps of the DU-10Mo foil sample surface are shown in Fig. 5. Below the platinum layer shown in Fig. 5b, there is a polycrystalline oxide-rich layer with cracks.

Several of the oxide-rich crystals are uranium rich, and others are molybdenum rich. This can be shown by comparing Figs. 5c and 5d. An EDS trace of one of the molybdenum-rich particles is shown in Figs. 5f and 5g. The trace shows the zone that is molybdenum rich that appears to be the core of this oxide-rich particle. This particle is not exclusively Mo as there is a substantial amount of uranium present as well. Looking at the oxygen trace in Fig. 5g, we can see that the oxide layer is ~450 nm thick in this region of the sample surface.

III.C. XPS Results

III.C.1. XPS Results for DU-8Mo Powder

Low-resolution XPS survey scans of the as-received DU-8Mo powder sample after undergoing a series of Ar sputtering cycles are shown in Fig. 6. As Fig. 6 shows,

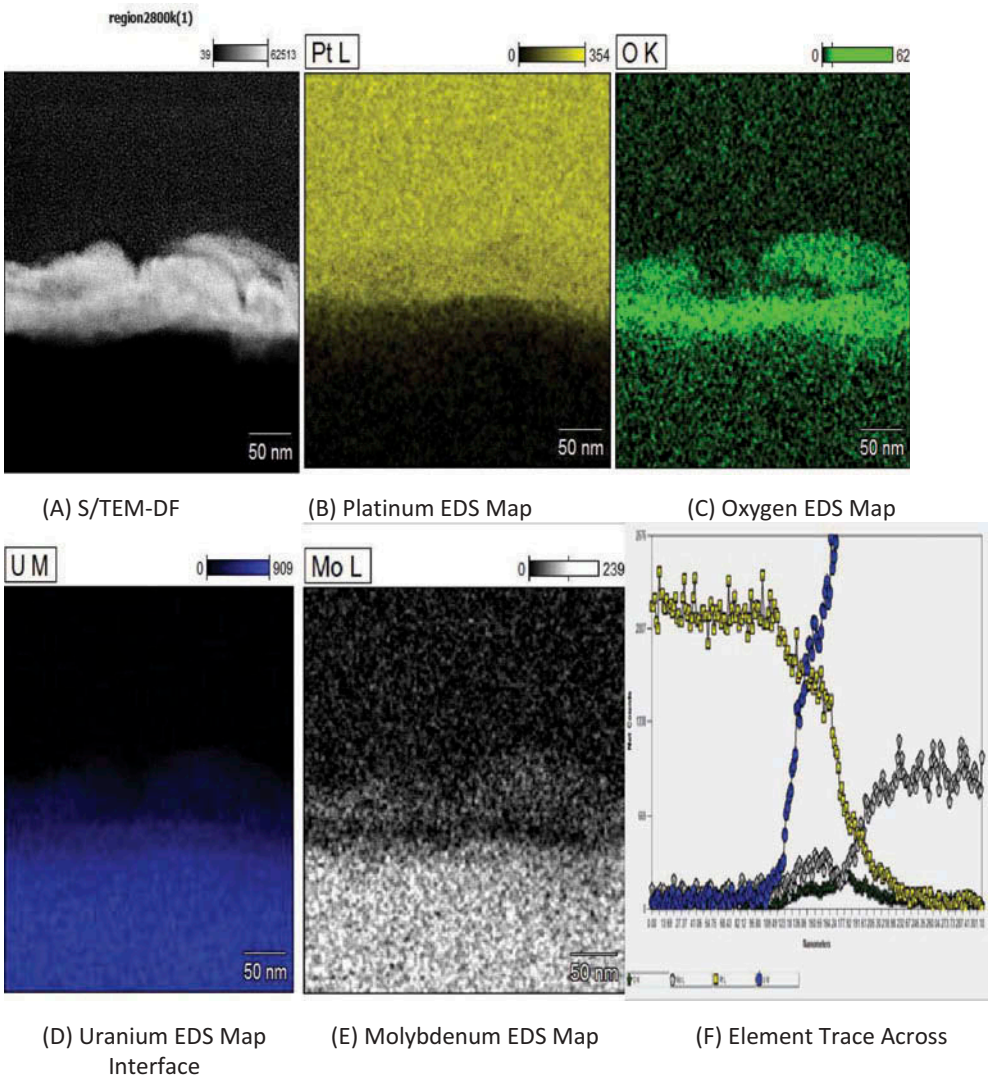

Fig. 3. High-resolution TEM analysis and EDS maps of as-received DU-8Mo powder sample.

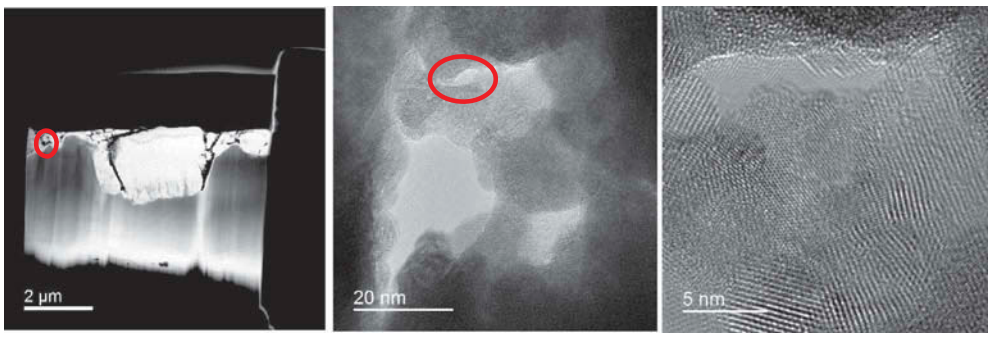

Fig. 4. TEM analysis of as-received DU-10Mo foil sample.

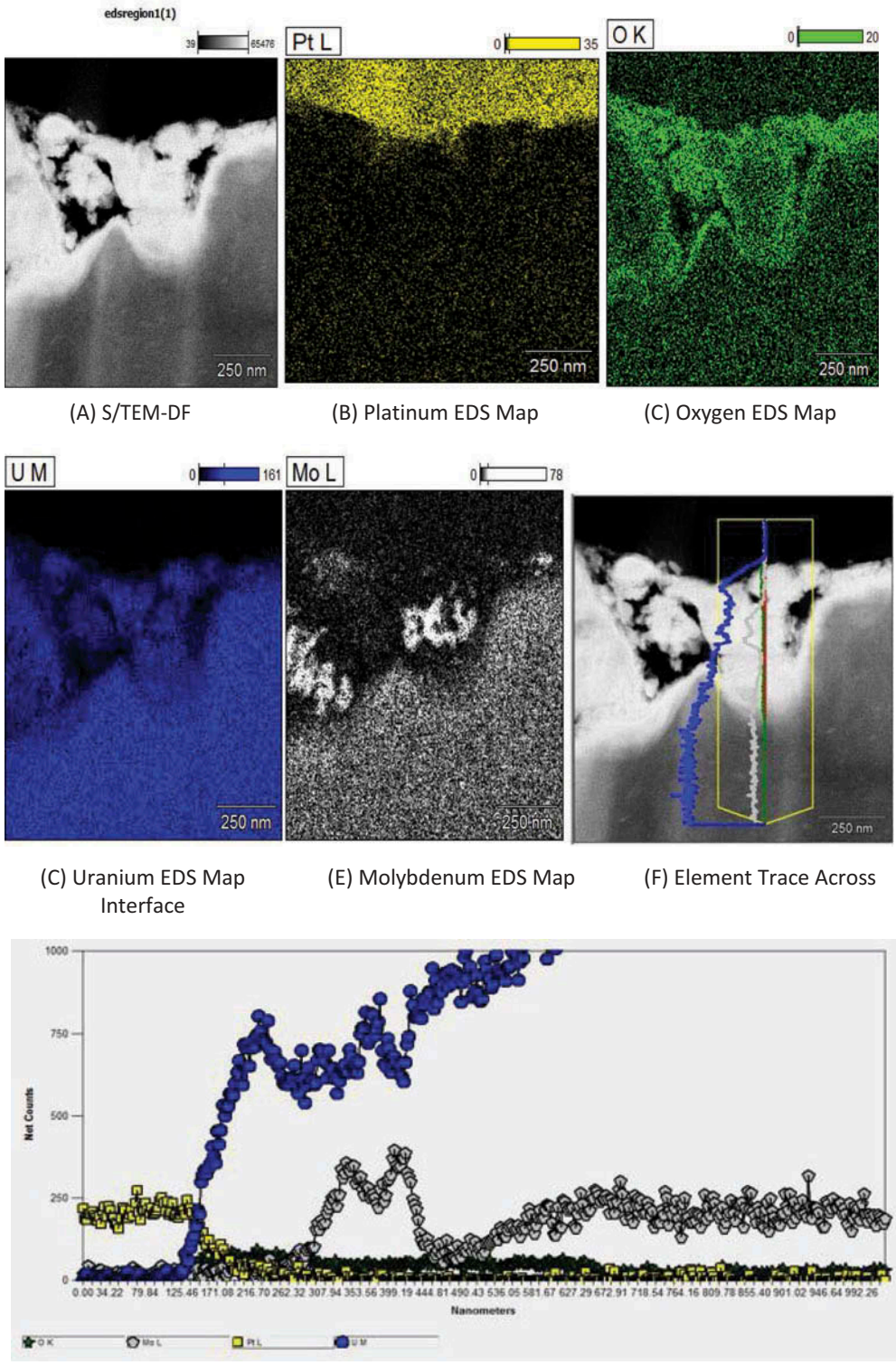

Fig. 5. TEM analysis and EDS maps of as-received DU-10Mo foil sample.

there is a substantial amount of oxygen and carbon on the surface as well as smaller amounts of uranium and molybdenum.

The surface chemical analysis of the as-received DU-8Mo powder sample is given in Table II as well as XPS results after argon ion sputtering for up to 20 min.

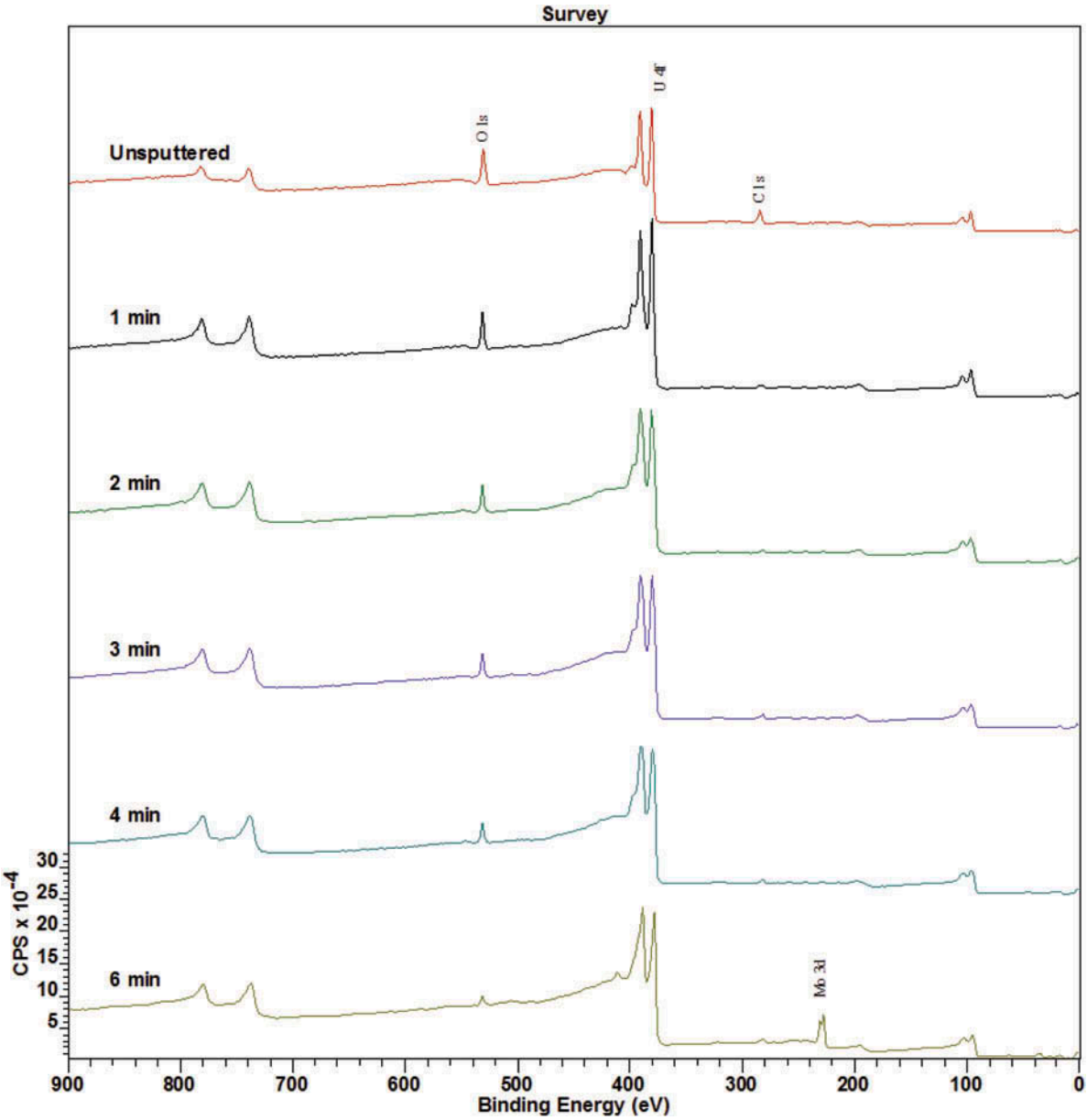

Fig. 6. Broad XPS scan of the as-received DU-8Mo powder sample.

TABLE II

XPS of the As-Received DU-8Mo Powder Sample

Elements	Relative Atomic Percentage								
	0 min	1 min	2 min	3 min	4 min	6 min	10 min	15 min	20 min
O	38.9	50.2	38.3	30.0	26.4	21.3	14.3	13.5	8.2
U	11.9	34.7	35.3	39.4	42.4	43.6	42.4	42.3	38.0
C	49.0	14.3	25.9	29.7	29.8	32.7	37.3	30.1	30.7
Mo	0.2	0.8	0.5	0.9	1.4	2.4	6.0	14.1	23.1

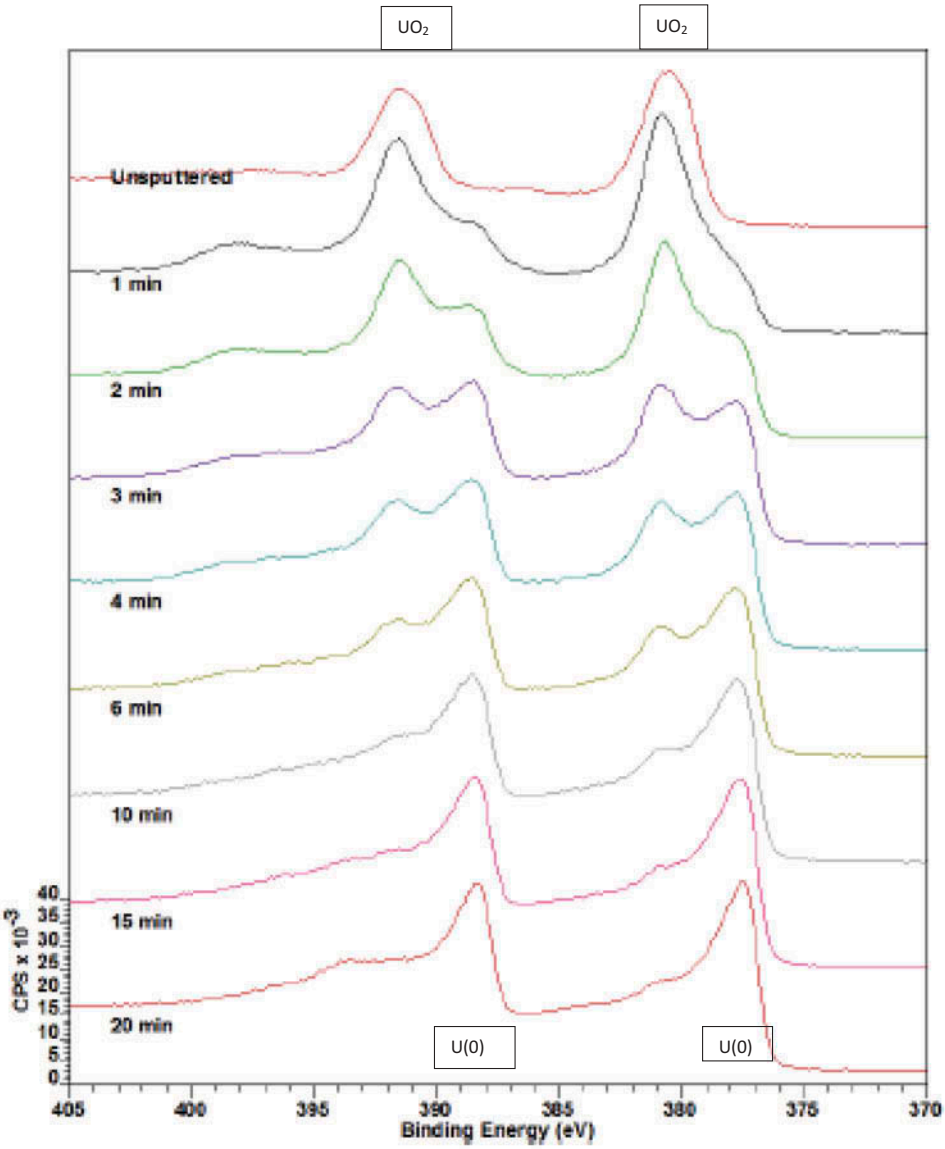

Fig. 7. High-resolution scan of the U-4f XPS peaks for the as-received DU-8Mo powder sample.

Keep in mind that about 20 to 40 nm of the surface is removed for each minute of argon ion sputtering. Carbon and oxygen surface contamination together are initially 87.9 at. % of the surface and decreases to 38.9 at. % with 20 min of argon ion sputtering. This is still a substantial amount of surface contamination. This sample also shows that as the surface carbon is removed by argon ion sputtering, the oxygen surface concentration increases and then decreases, suggesting that the initial surface is either graded or heterogeneous as we have seen with the EDS maps.

High-resolution scans of the U-4f XPS peaks between 375- and 400-eV binding energy are shown in Fig. 7. Here, we see that the as-received U-Mo alloy is oxidized at the surface with UO_2 as the predominant species. As the surface is sputtered, the oxide is slowly removed until it plateaus at the 15-min mark. After 1 min of argon ion sputtering, we see the first signs of metallic uranium U(0) with a binding energy of 388.5 eV (4f 5/2) and 377.5 eV (4f 7/2) and a constant decrease in uranium oxide peaks. However, even after 20 min of argon ion sputtering, there is still an oxide at the DU-8Mo powder surface.

Figure 8 shows the high-resolution scan of the Mo-3d peak for the as-received DU-8Mo powder sample as a function of argon ion sputtering time. There is no evidence of Mo on the surface of the as-received sample. The first sign of Mo was observed after 6 min

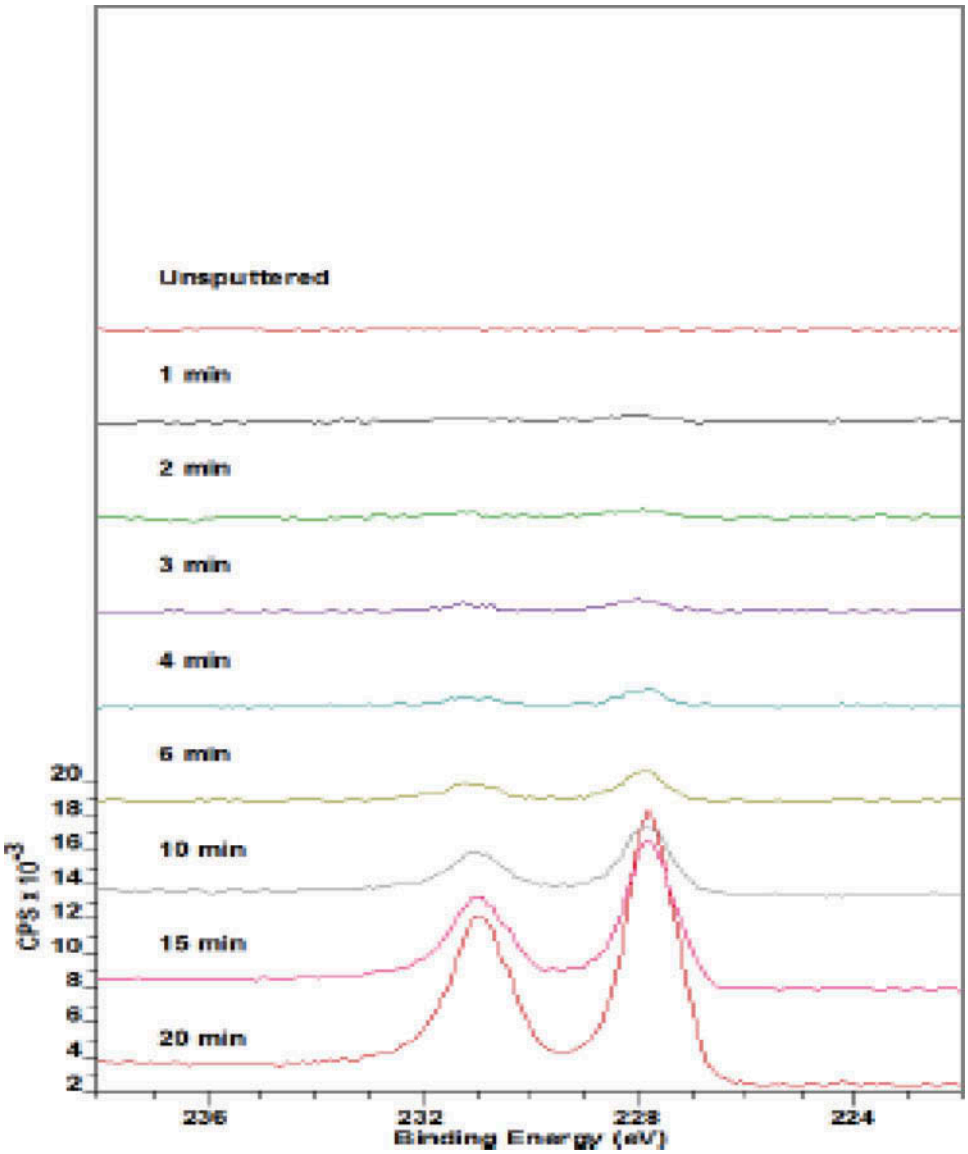

Fig. 8. High-resolution scan of the Mo-3d peak for the as-received DU-8Mo powder sample.

of argon ion sputtering where a Mo-3d peak was detected at a binding energy of ~228 eV, which is distinctive of unoxidized Mo species. The same peak grows significantly as sputtering is performed for an additional 14 min (20 min of total sputter time).

Figure 9 shows the high-resolution XPS scan of the O-1s region. Initially, a peak at 530-eV binding energy with a shoulder at 532 eV was observed on the surface. Interestingly, the same peak was observed ~1 eV higher with the shoulder removed after sputtering. The weak shoulder at the higher binding energy region is attributed to adsorbed O_2 or H_2O mainly coming from the atmosphere. The main peak is assigned to oxygen of the UO_2 surface species. The peak shift with argon ion sputtering is a curious phenomenon that was also observed and discussed in more detail by Ilton and Baugus[9] and Senanayake et al.[10] Briefly, the binding energy shift of the oxide O-1s peak is attributed to a change in the Fermi energy of the surface due to formation of a suboxide species. Oxidized uranium transitions to an n-type semiconducting material as oxygen gets depleted from the initial UO_2 lattice.[10]

Figure 10 shows the high-resolution scan of the C-1s region. The most intense peak at ~284 eV is assigned to a C-C bond from adventitious sources. C-O and COO species, typical of adventitious contaminations, are also observed on the unsputtered surface. These species were significantly removed after sputtering. With additional

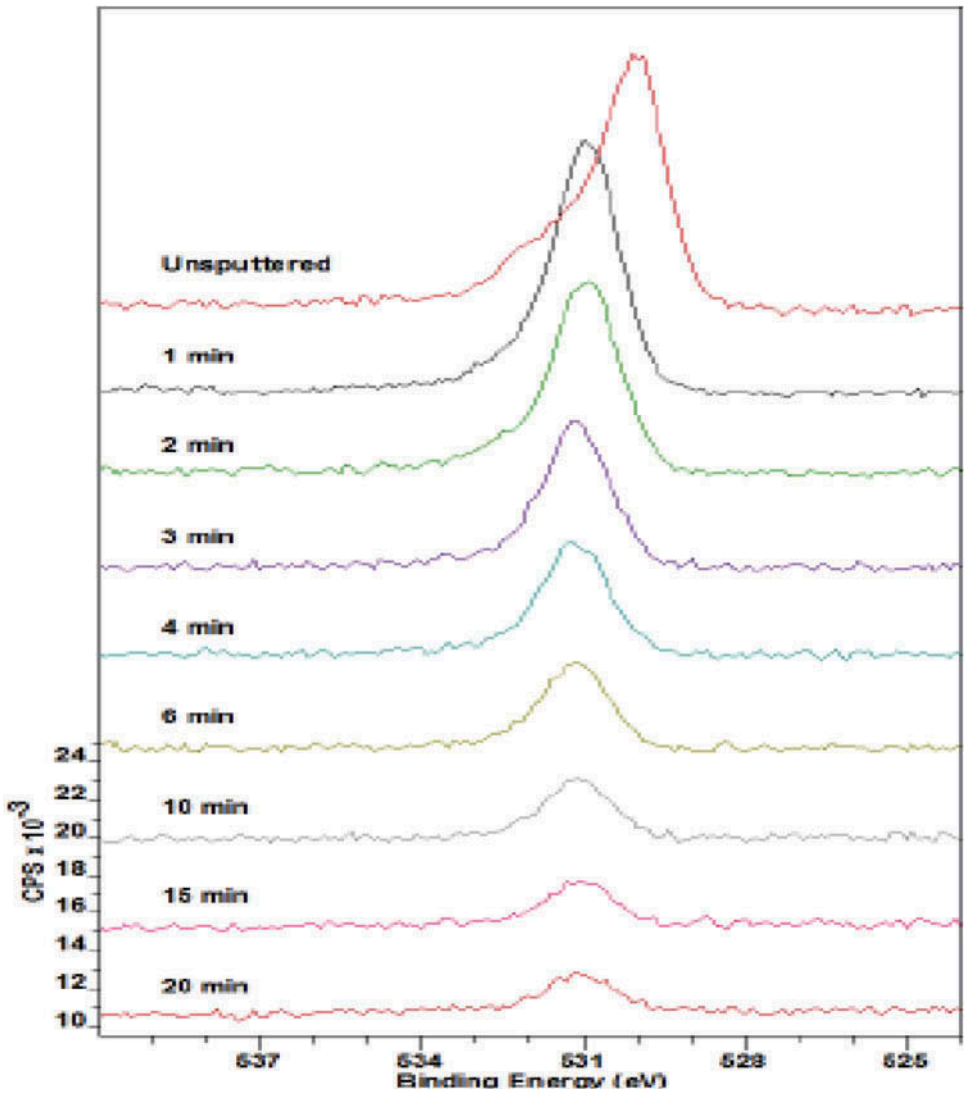

Fig. 9. High-resolution scan of the O-1s peak for the as-received DU-8Mo powder sample.

sputtering, the peak shifts to a binding energy of 282 eV, which is indicative of a carbide being formed. Interestingly, the carbide peak seems to increase in intensity as the surface is sputtered up until the 10-min mark. This peak's intensity did not change much as the sample is sputtered further. Formation of metallic carbide during sputtering is not unusual on metals and alloys.[11,12] We have observed this in our analysis of oxidized Mo powders and wires prior to the DU-Mo alloys (data not presented). In the current study, the presence of U in the alloy complicates interpretation of this carbide peak. It is also possible that carbon can bind with uranium atoms to form UC. Oxygen atoms are very favorably incorporated as diluted atoms in the UC lattice, confirming the easy oxidation of UC. The oxygen atoms preferably occupy a carbon substitution site or the carbon site of a U-C bivacancy.[13] One way to confirm the presence of UC is to analyze the high-resolution U-4f spectrum and look for peaks that would correspond to UC species (at binding energy equal to ~278 eV).

Unfortunately, this binding energy lies in close proximity to metallic U, which is also observed after sputtering for 1 min. We cannot confirm the presence of UC, with absolute certainty, mainly from the existence of the peak at 278 eV. However, when we look at the relative amount of carbon atoms in the carbide species as compared to Mo at the first instance that the carbide species appeared (after 1 min of sputtering), the amount of carbon atoms forming the carbide is significantly higher than the total Mo, e.g, peak intensity ratio of 7:0.8, and the carbide peak intensity is at least 50% of the total C-1s peak. This suggests that there are other sources of metal carbide, most

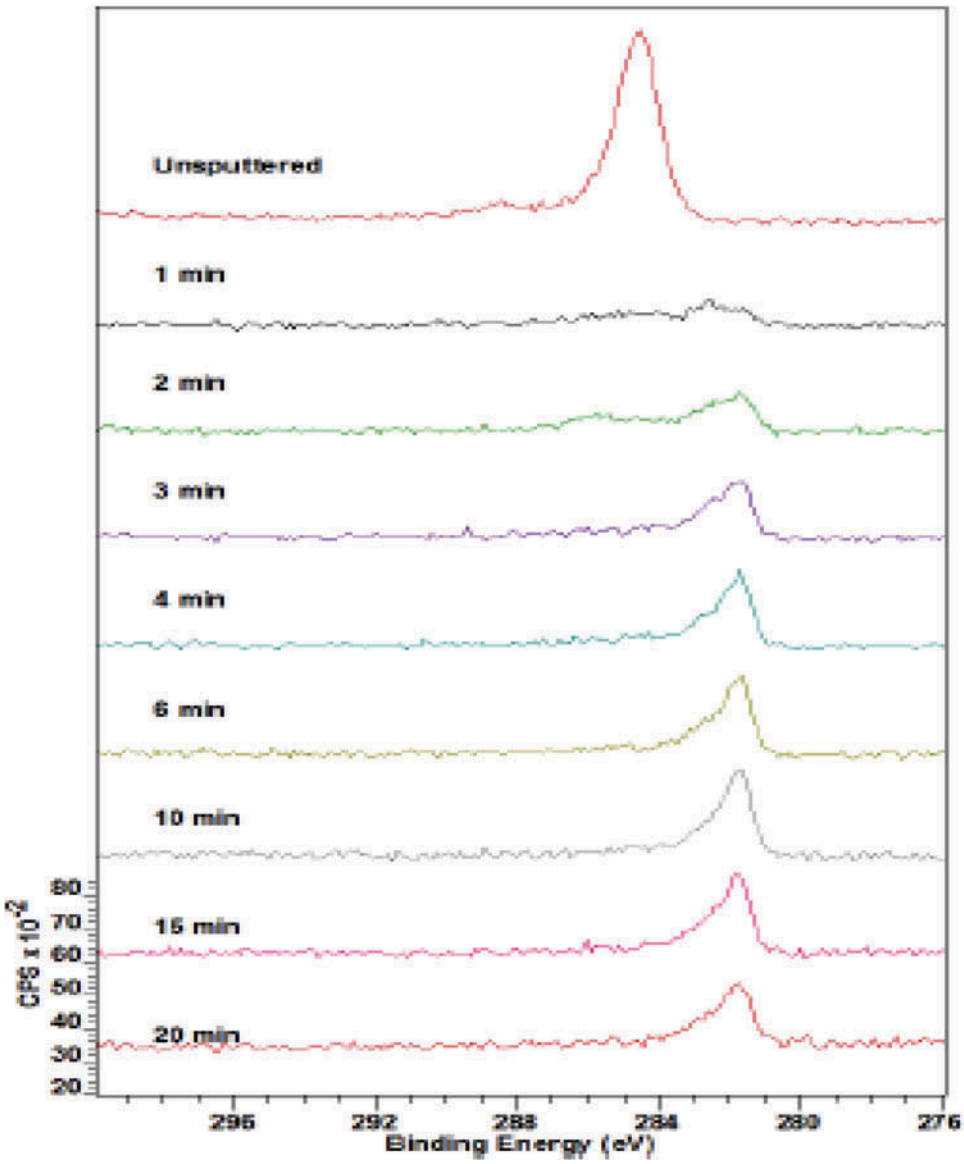

Fig. 10. High-resolution scan of the C-1s peak for the as-received DU-8Mo powder sample.

likely MoC, contributing to the peak at ~282 eV that was attributed to the presence of UC.

III.C.2. XPS Results for DU-10Mo Foil

Figure 11 shows the XPS of the as-received DU-10Mo foil sample. It shows that there is a substantial amount of oxygen and carbon on the surface as well as smaller amounts of calcium and uranium. The surface chemical analysis of the as-received DU-10Mo foil sample is given in Table III as well as XPS results after argon ion sputtering cycles for 30s and for 3 min.

The as-received sample has 91.12 at. % carbon and 7.6 at. % oxygen on the surface. Small amounts of calcium, uranium, molybdenum, and zirconium are also observed prior to sputtering. After argon ion sputtering for 30 s, the surface carbon contamination is reduced to 83.8 at. %, and oxygen is increased to 11.1 at. %. With 3 min of argon ion sputtering, the carbon is further reduced to 70.52 at. %, and the oxygen is further increased to 16.79 at. %. The first significant amounts of uranium and molybdenum are observed only after 3 min of argon ion sputtering with the appearance of zirconium at 30 s and slightly more zirconium at 3 min of argon ion sputtering while the amount of calcium is smaller at 3 min than at 30 s of

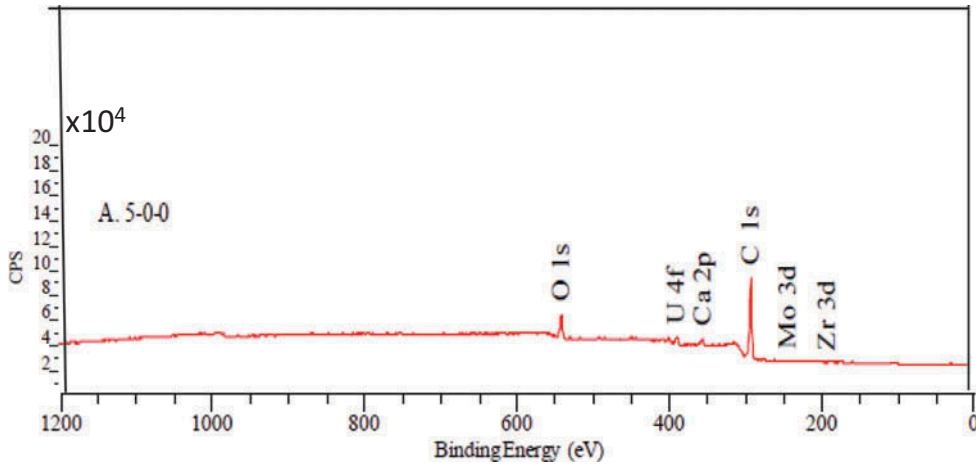

Fig. 11. XPS of as-received DU-10Mo foil sample.

TABLE III

XPS Surface Analysis for As-Received DU-10Mo Foil Sample

Etch Time = 0 s			
Peak	Position Binding Energy (eV)	Atomic Concentration (%)	Mass Concentration (%)
Ca-2p	347.0	0.96	2.88
O-1s	530.9	7.60	9.13
U-4f	380.5	0.33	5.83
C-1s	285.7	91.12	82.16
Etch Time = 30 s			
Peak	Position Binding Energy (eV)	Atomic Concentration (%)	Mass Concentration (%)
Ca-2p	347.0	1.78	3.79
O-1s	530.6	11.10	9.41
U-4f	380.2	2.21	27.95
C-1s	284.7	83.80	53.37
Mo-3d	282.3	0.45	2.28
Zr-3d	182.8	0.66	3.19
Etch Time = 180 s			
Peak	Position Binding Energy (eV)	Atomic Concentration (%)	Mass Concentration (%)
Ca-2p	347.0	1.45	1.70
O-1s	530.9	16.79	7.89
U-4f	380.3	8.15	57.00
C-1s	284.4	70.52	24.88
Mo-3d	227.9	1.78	5.01
Zr-3d	182.9	1.31	3.51

argon ion sputtering. There are three things that are surprising about this sample: (1) There are both calcium and zirconium in the sample, (2) there is a large amount of carbon and oxygen that remains after 3 min of argon ion sputtering, and (3) there is a very large amount of carbon surface contamination.

High-resolution scans of the U-4f XPS peaks between 375- and 400-eV binding energy are shown in Fig. 12. Here, we see that the as-received sample and the 30-s argon ion sputtered sample have uranium oxide UO_2 at the surface, which is less in the as-received sample than in the 30-s sputtered sample, which seems contrary to the logic of argon ion sputtering cleaning the surface. After 3 min of argon ion sputtering and Gaussian peak reconstruction, we see the first signs of metallic uranium U(0) with a binding energy of 388.5 eV (4f 5/2) and 377.5 eV (4f 7/2).

This completes the analysis of the as-received samples of DU-8Mo powder and DU-10Mo foil samples. In an attempt to clean up these highly contaminated surfaces, hydrogen treatment of the surfaces was performed. Section III.C.3 discusses the TEM and XPS results for these hydrogen treatments.

III.C.3. Results of Hydrogen Treatment

The XPS results for the DU-10Mo foil sample after 4 h of treatment in 4.901% hydrogen at 3 bar(a) and at different temperatures are shown in Fig. 13. With higher temperatures, the XPS results show more uranium, and less carbon is observed. The XPS surface chemical analysis for these 4-h treatments is given in Table IV for the samples given in Fig. 13. From Table IV, we see that the surface carbon is reduced from 91 to 40 at. % while the surface oxygen is increased from 7.6 to 44.4 at. % and the surface uranium is increased from 0.22 to 14.37 at. %.

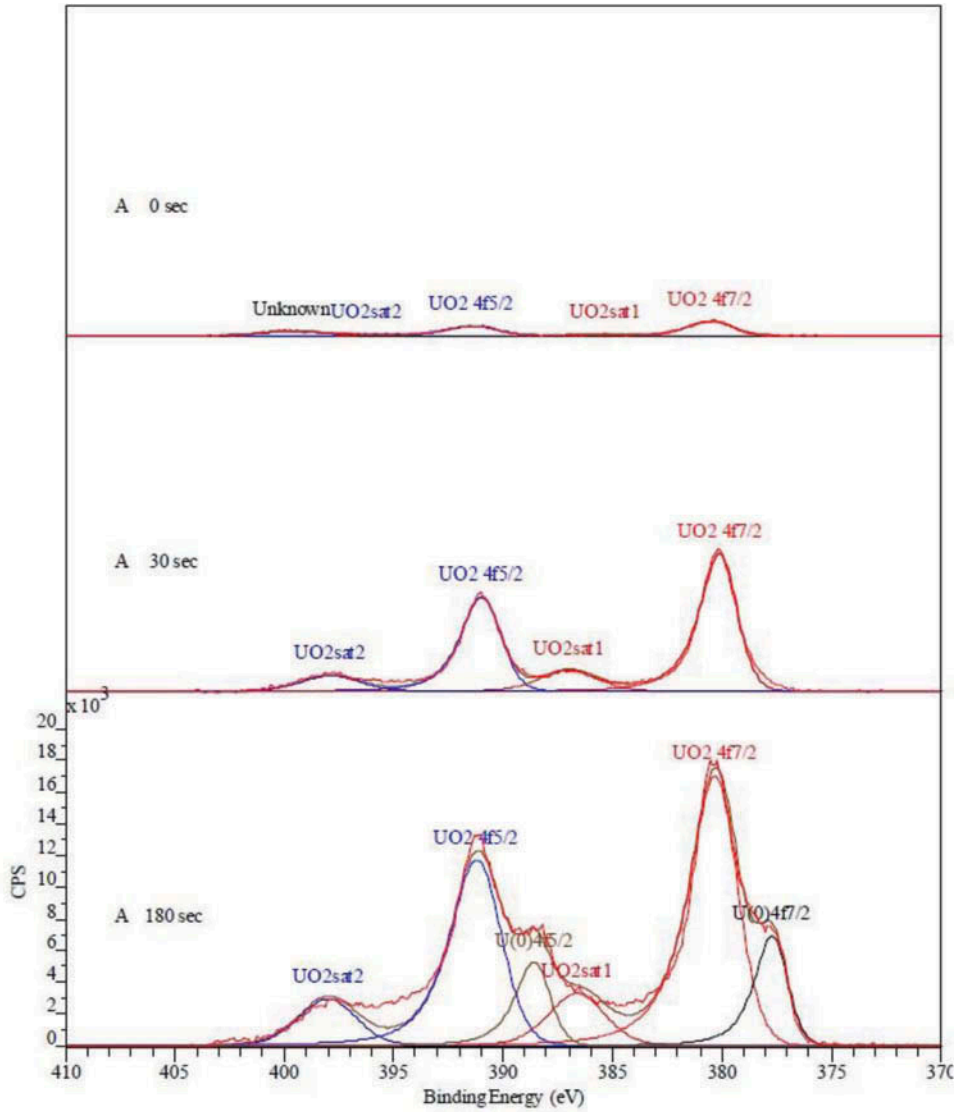

Fig. 12. XPS spectra of the U-4f peak in the as-received DU-10Mo foil sample.

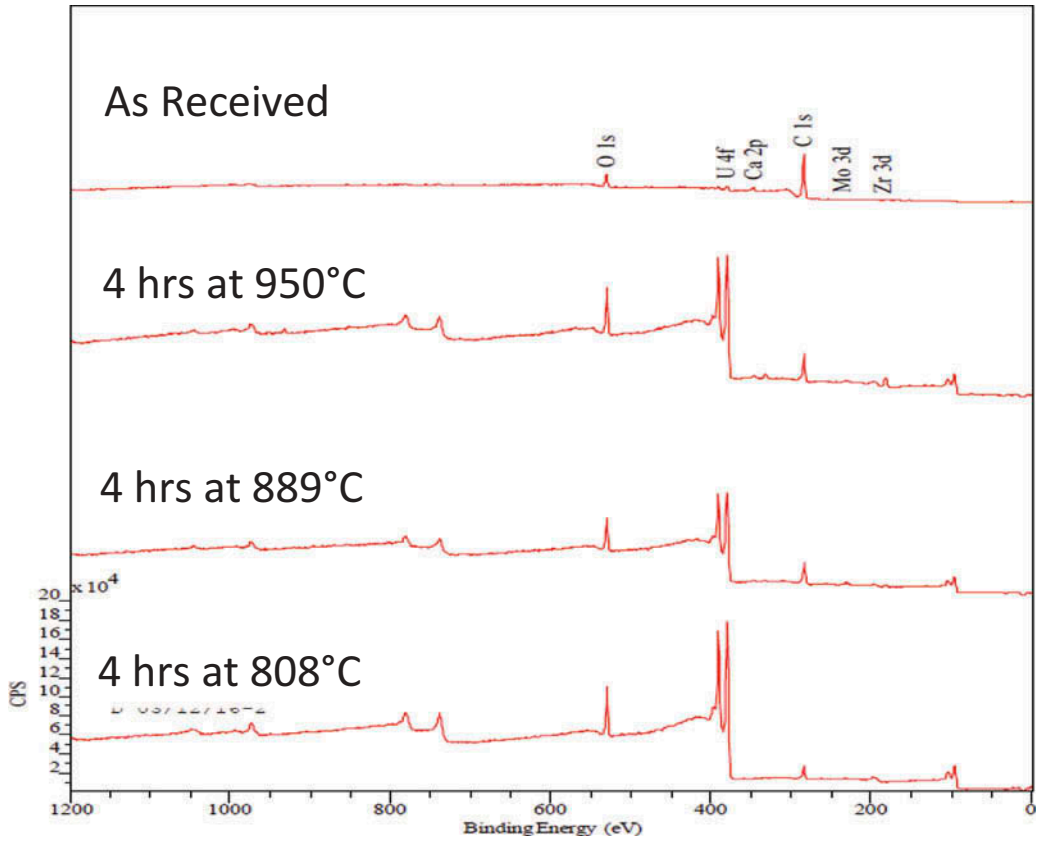

Fig. 13. XPS of DU-10Mo foil treated 4 h in 4.910%H_2/Ar mixture at 0.1 SLPM and 3.0 bar(a).

TABLE IV

XPS Surface Chemical Analysis of DU-10Mo Foil Treated 4 h in 4.910%H_2/Ar Mixture at 0.1 SLPM and 3.0 bar(a)

Peak	As-Received	4 h 3 bar(a) 5%H_2 at 808°C	4 h 3 bar(a) 5%H_2 at 889°C	4 h 3 bar(a) 5%H_2 at 950°C
O-1s	7.60	28.86	25.66	44.38
U-4f	0.33	7.05	6.42	14.37
C-1s	91.12	60.58	64.89	40.30
Mo-3d	—	0.76	1.12	0.81
Zr-3d	0	2.75	0.90	0.13
Ca-2p	0.96	—	1.02	—

Molybdenum, zirconium, and calcium are small in all of these 4-h samples. High-resolution scans of (1) the Mo-3d peak at a binding energy of 332 eV shows that there is MoO_3 on top of Mo(0) species in the surface at all temperatures and (2) the Zr-3d peak at a binding energy of 182 eV shows that Zr on the surface is oxidized to ZrO_2. It is not at all clear where the zirconium comes from in this sample. It may be due to a poorly selective chemical process where the Zircaloy cladding was not completely removed from reprocessed fuel used in making this DU-10Mo foil sample.

In frustration, to find a way to remove the surface contamination from the DU-10Mo foil sample, a 96-h exposure to 3 bar(a) of 4.910% H_2 at 950°C was performed. The XPS results are shown in Fig. 14 and Table V. High-resolution scans of the Zr-3d peak showed that Zr was observed on the surface and was not completely removed with 25 min of argon ion sputtering. High-resolution scans of the U-4f (7/2) peak at 378 eV shows that after 5 min of argon ion sputtering, the presence of metallic U(0) appears; however, further sputtering for an additional 20 min did not significantly remove the uranium oxide layer, as indicated by this uranium peak remaining at a constant size and the high-resolution scan of the O-1s peak at 531 eV. The appearance of the metallic U-4f (7/2) peak is more likely due to preferential sputtering of O atoms resulting in reduction of UO_2 and not from exposing the underlying metallic layer of uranium. A shift to lower binding energy was observed after a light 30-s sputtering with argon ions. This is due to the removal of adsorbed O and moisture (H_2O), which are typically observed at binding energies higher than that of the oxide species. The high-resolution

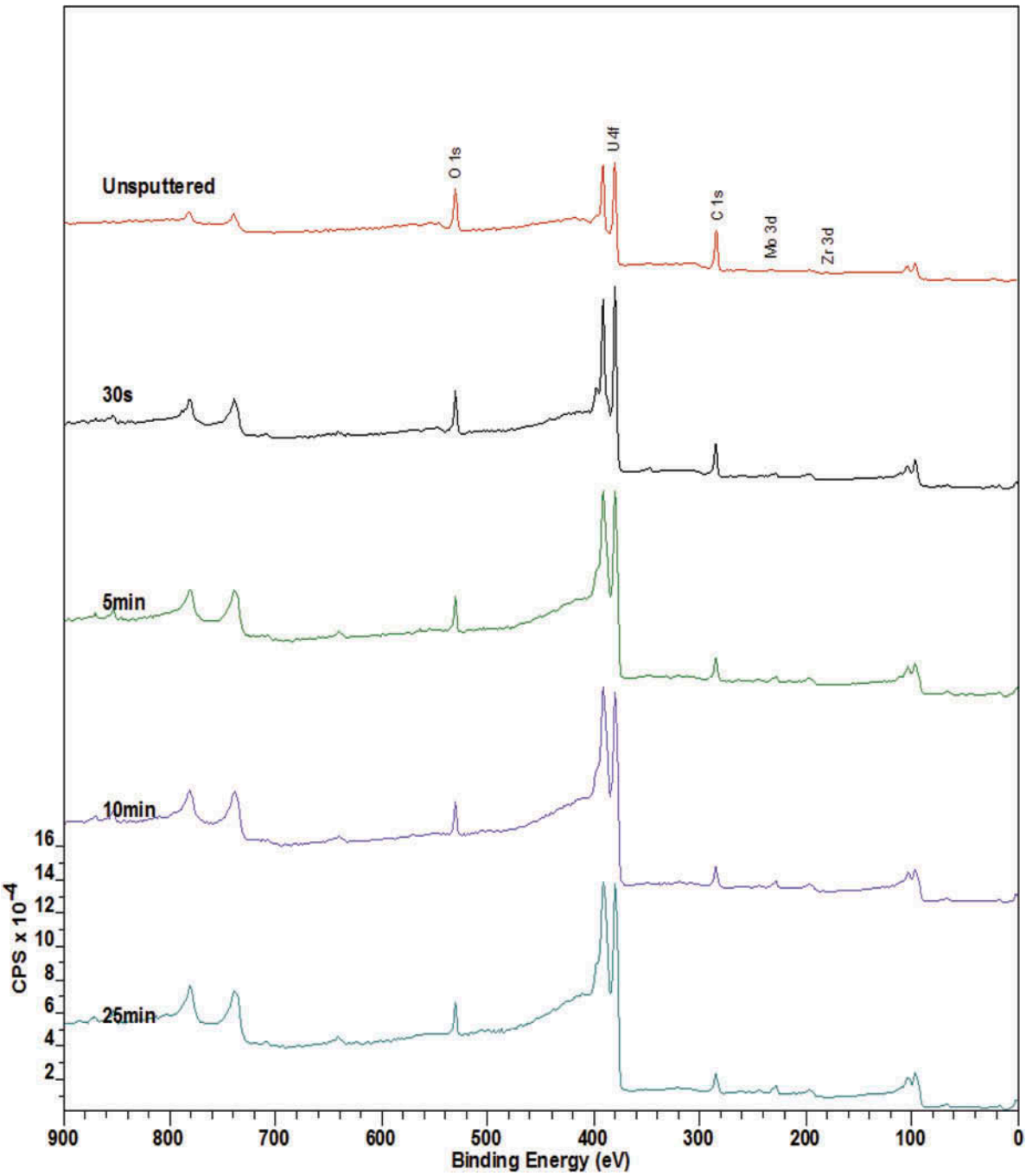

Fig. 14. XPS of DU-10Mo foil treated 96 h in 4.910%H_2/Ar mixture at 0.1 SLPM and 3.0 bar(a).

scan of the C-1s peak shows a large amount of adventitious carbon even after 25 min of sputtering and that a carbide species was formed after 5 min of argon ion sputtering. The sample after 96 h of H_2 treatment and 25 min of argon ion sputtering is a much darker black in color indicative of UC.

The XPS results for 96-h samples at 889°C and 808°C, which are not provided here, show substantially the same results as those for the 950°C sample and that subsequent argon ion sputtering was also unsuccessful in removing surface contamination of carbon and oxygen from this DU-10Mo foil sample.

The results for H_2 treatment for the DU-10Mo foil sample show that the surface contamination of carbon and oxygen is not removed by this 96-h hydrogen treatment and that substantial surface contamination remains after as long as 25 min of argon ion sputtering. The amount of carbon and

TABLE V

XPS Surface Chemical Analysis of DU-10Mo Foil Treated 96 h in 4.910%H_2/Ar Mixture at 0.1 SLPM and 3.0 bar(a) and 950°C

Element	Relative Atomic Percentage			
	Unsputtered	30 s	5 min	25 min
O	27.1	28.4	23.0	22.8
U	5.5	13.1	18.6	26.8
Ca	1.0	1.9	1.1	[a]
C	65.7	55.8	55.6	48.0
Mo	0.5	0.5	1.2	2.4
Zr	0.2	0.2	0.4	[a]

[a]Ca-2p and Zr-3d region scans were not performed after 5 min since the peaks were almost negligible.

oxygen that remains after 25 min of argon ion sputtering suggests that the surface contamination layer is 1 to 10 μm thick on this DU-10Mo foil sample.

IV. CONCLUSIONS

The DU-8Mo powder and DU-10Mo foil samples have surface contamination that is hundreds to thousands of nanometers thick of oxygen and carbon in different ratios. The DU-8Mo powder sample that has been stored in an inert atmosphere has less carbon and more oxygen at the surface than the DU-10Mo foil sample. This surface contamination has not been removed by up to 20 min of argon ion sputtering nor with hydrogen heat treatments for 96 h at 950°C. It is worth considering that the Gibbs free energy of formation of UO_2 is −1085 kJ/mol (Ref. 14) and that of U_2O_3 is −1223 kJ/mol, some of the most negative Gibbs free energies for oxides in the periodic table and as a result the most stable oxides. In the electrochemical context, the oxidation of uranium metal to U^{+3} has a standard half-cell potential[15] of −1.798 V, which is more negative than that of aluminum by 0.136 V, indicating that U_2O_3 is a more stable oxide than Al_2O_3, which is not reduced by hydrogen. The Gibbs free energy of formation of U_2C_3 is −183 kJ/mol (Ref. 16) corresponding to a stable carbide as well.

Given the tenacious surface contamination in both of these samples, putting a ZrN coating on the contaminated U-Mo surface will be problematic as the crystal structure and unit-cell spacing of ZrN are very different from that of the oxide or carbide making the ZrN coating of these surface-contaminated DU-Mo samples poorly attached and subject to spalling and preventing a hermetic seal of the DU-Mo substrate even before it is subject to massive swelling due to the accumulation of fission gases.

Acknowledgments

This work was graciously funded by INL under contract award number 150387 of the Global Threat Reduction Initiative, United States High Performance Research Reactor Fuel Development: Microstructure and Surface Characterization, project number 25228.

ORCID

Terry A. Ring http://orcid.org/0000-0001-7368-3648
Douglas Crawford http://orcid.org/0000-0001-5639-7885
Dennis Keiser http://orcid.org/0000-0003-3387-9026
Daniel Wachs http://orcid.org/0000-0002-9239-3424

References

1. M. K. MEYER et al., "Irradiation Performance of U-Mo Monolithic Fuel, Nuclear Engineering and Technology," **46**, *2*, 169 (Apr. 2014); https://doi.org/10.5516/NET.07.2014.706.
2. R. M. WILLARD and A. R. SCHMITT, "Irradiation Swelling, Phase Reversion and Intergranular Cracking of U-10wt%Mo Fuel Alloy," NAA-SR-8956, Atomics International (1964).
3. A. A. SHOUDY, W. E. McHUGH, and M. A. SILLIMAN, "The Effect of Irradiation Temperature and Fission Rate on the Radiation Stability of Uranium-10 Wt% Molybdenum Alloy," *Radiat. Damage Reactor Mater.*, **46**, *1*, 133 (1963).
4. "Various Materials Crystal Structures and Lattice Constants" Wikipedia website (Aug. 2016); https://en.wikipedia.org/wiki/Uranium; https://en.wikipedia.org/wiki/Molybdenum; https://en.wikipedia.org/wiki/Zirconium; https://en.wikipedia.org/wiki/Silicon; https://en.wikipedia.org/wiki/Aluminum.

5. S. SAARINENM, "Isotopically Enriched Nitrides for Nuclear Power" (2102); http://www.diva-portal.se/smash/get/diva2:551031/FULLTEXT01.pdf (current as of Aug. 2016).

6. *Metallurgical Coatings and Thin Films*, G. E. McGUIRE, S. HOFMANN, and B. D. SARTWELL, Eds., p. 262, Elsevier Science (1992).

7. M. BALACEANU et al., "Surface Chemistry of Plasma Deposited ZrC Hard Coatings," *J. Optoelectron. Advan. Mater.*, **7**, *5*, 2557 (Oct. 2005); http://joam.inoe.ro/arhiva/pdf7_5/Balaceanu.pdf (current as of Aug. 2016).

8. C. B. VINCENT, *Handbook of the Elements and Native Oxides*, XPS International, Inc. (1999); http://www.xpsdata.com/XI_BE_Lookup_table.pdf (current as of Aug. 2016).

9. E. S. ILTON and P. S. BAUGUS, "XPS Determination of Uranium Oxide States," *Surf. Interface Anal.*, **43**, 1549 (2011); https://doi.org/10.1002/sia.3836.

10. S. D. SENANAYAKE et al., *J. Vac. Sci. Technol. A*, **23**, 1078 (2005); https://doi.org/10.1116/1.1881637.

11. P. SELVAM, B. VISWANATHAN, and V. SRINIVASAN, "Note on the Formation of Surface Carbides," *J. Elect. Spectrosc. Relat. Phenom.*, **50**, 277 (1990); https://doi.org/10.1016/0368-2048(90)87071-U.

12. J. S. PAN et al., "Argon Incorporation and Silicon Carbide Formation During Low Energy Argon-Ion Bombardment of Si(100)," *J. Appl. Phys.*, **79**, 2934 (1996); https://doi.org/10.1063/1.361289.

13. M. FREYSS, "First-Principles Study of Uranium Carbide: Accommodation of Point Defects and of Helium, Xenon, and Oxygen Impurities," *Phys. Rev. B*, **81**, 014101 (Jan. 4, 2010); https://doi.org/10.1103/PhysRevB.81.014101.

14. "NIST Chemistry Web Book," National Institute of Standards and Technology; www.nist.gov/webbook/ (current as of Aug. 2016).

15. *CRC Handbook of Chemistry and Physics*, 87th ed., D. R. LIDE, Ed., CRC Press, Boca Raton, Florida, ISBN 0-8493-0487-3 (2006).

16. H. HOLLECK and H. KLEYKAMP, *U Uranium: Uranium Carbides*, Springer Science and Business Media (2014).